Optical Engineering

OpticalEngineering.SPIEDigitalLibrary.org

Topology and parametric optimization based lightweight design of a space reflective mirror

Guang Liu
Liang Guo
Xintong Wang
Qingwen Wu

SPIE.

Guang Liu, Liang Guo, Xintong Wang, Qingwen Wu, "Topology and parametric optimization based lightweight design of a space reflective mirror," *Opt. Eng.* **57**(7), 075101 (2018), doi: 10.1117/1.OE.57.7.075101.

Topology and parametric optimization based lightweight design of a space reflective mirror

Guang Liu,[a,b] Liang Guo,[a,*] Xintong Wang,[a,b] and Qingwen Wu[a]
[a]Chinese Academy of Sciences, Changchun Institute of Optics, Fine Mechanics and Physics, Changchun, China
[b]University of Chinese Academy of Sciences, Beijing, China

Abstract. For large space telescopes, the design of lightweight primary mirrors with an acceptable level of optical performance is a challenge. A parametric optimization method based on topology optimization of the basic configuration of the mirror is proposed. A finite-element model of the mirror is generated with linear shell elements, and the optimal distribution of the material is obtained using the continuum topology optimization technique. The lightweight ribs are grouped according to the results of topology optimization results. The design of experiment method is used to pick out the key factors for parametric optimization. The RMS value of the surface shape error of the mirror and the total mass of the mirror are treated as the objective merit functions, and the first-order natural frequency of the mirror is taken as a constraint for parametric optimization. Results show that the local stiffness of the mirror is significantly affected by the thicknesses of the ribs at the corresponding positions. The optimum mirror design obtained using our optimization method is compared with the initial design, and the comparison shows superior optical performance for the optimized mirror. [DOI: 10.1117/1.OE.57.7.075101]

Keywords: lightweight mirrors; optomechanics; space optics; optimization design.

Paper 180061 received Jan. 11, 2018; accepted for publication Jun. 12, 2018; published online Jul. 5, 2018.

1 Introduction

Large-aperture primary mirrors have emerged as a popular way to meet the increasing system angular resolution requirements for space telescope systems. However, increasing the diameter of such a mirror aggravates the deformation caused by the self-weight of the mirror under gravity, which in turn affects the accuracy of the optical surface of the mirror and eventually leads to degradation of the image quality. In addition, the launch costs are directly related to the mirror mass. The focus has therefore largely been on developing lightweight, large-aperture mirrors to negate both of these disadvantages. Lightweight mirror designs are very important to maintain the quality of the optical surface of large-caliber space mirrors and to reduce mission costs. The design of lightweight mirrors has therefore become a key focus in the design of large-space telescope optical systems.[1]

Methods of reducing the weight of such mirrors include the use of lightweight materials and lightweight mirror structure designs. Among the possible lightweight materials, silicon carbide (SiC) has a lower density, higher specific stiffness, better thermal conductivity, and other physical and mechanical advantages over traditional materials, such as lithium-aluminum-silicon glass ceramic (Zerodur®) and beryllium. Its development has become a source of much progress in the design of space mirrors.[2,3]

Topology optimization and parametric optimization methods are widely used to assist in the design of lightweight space mirrors. There is a lot of available literature on such design optimization techniques. Structural optimization of a 1.2-m-diameter Zerodur space mirror was carried out by Sahu using the OptiStruct tool of HyperWorks 12 to minimize the mass and constrain optical aberrations.[4] Instead of the root mean square (RMS) surface error, the defocus, coma, and trefoil aberrations were taken as the constraints. Two load scenarios, one for the axial and the other for the lateral inertial force on the mirror, were examined for each design case. However, the final design was not feasible to manufacture using the milling process typical for traditional open-back glass mirrors. The optimized mirror would have to be manufactured in parts and then combined by frit-bonding. Park et al.[5,6] presented a study of the topology optimization of the primary mirror of a multispectral camera under self-weight and polishing pressure loading. A measurement of the Strehl ratio was the objective merit function, and the total mass of the primary mirror was the constraint in the optimization problem. Results show that the optimal mirror had good optical properties with low mechanical deflection. A lightweight design of a primary mirror for a large-aperture space telescope derived using a topology optimization technique was proposed by Liu et al.[7] With explicit parameterization introduced, a tree-like mirror configuration was proposed. The optical performance of the proposed mirror was compared with two classical lightweight mirrors, and results showed the superiority of the mirror configuration. An optimum lightweight design for a Zerodur primary mirror with an outer diameter of 566 mm was presented by Chen et al.[8] Two boundary conditions (polishing and vertical-axis gravitational effects, and self-weight deformation of the horizontal-axis mirror) were chosen. The peak-to-valley (PV) value of the optical path difference due to the deformation of the mirror surface under these two scenarios was set as the constraint. The

*Address all correspondence to: Liang Guo, E-mail: guoliang@ciomp.ac.cn

0091-3286/2018/$25.00 © 2018 SPIE

optimization object was set to minimize the total mass of the mirror. Compared with the initial design (without lightweight cells in the rear face), the lightweight ratio of the final design increased from 56% to 66%, and superior optical performance and stiffness were achieved. Design optimization of a 1-m Zerodur lightweight mirror with pockets on the back surface and three square bosses on the rim was presented by Kihm and Yang.[9] With this method, the mirror design and the flexure design were separated into two independent problems to be parallel-processed without interfering with each other. Due to the multiple constraints and targets defined in their work, a multiobjective genetic algorithm (MOGA) was used for the optimization. Other research on the topology and parametric optimization of space mirrors can be found in Refs. 10–12.

The topology optimization methods for space mirrors described in previous research generally start from a continuum solid blank attempt to control the RMS distortion of the mirror surface. However, this method has some inherent drawbacks. If the solid blank is directly used as the optimization object, the design variable is too large, and the process to find a solution will become very complicated with high calculation costs. Additionally, the lightweight mirrors obtained using this method are usually very complex, and therefore difficult or even impossible to manufacture using existing technology. In the case of the parametric optimization of mirrors based on their basic configuration, all ribs are generally created with the same thicknesses or grouped according to their geometric distribution. The optimal results are therefore always limited by the way the ribs are grouped. In fact, not all ribs contribute equally to the load distribution. The question of how to rationally group the ribs of the mirror becomes a key factor in the final optimization results. In this paper, a parametric optimization method based on topology optimization of the basic configuration of the mirror is proposed. First, since the mirror is designed as a web-skin-type structure, it is possible to build a finite-element model using linear shell elements. Second, the finite-element model obtained in the first step is examined using topology optimization, and the optimal material distribution of the ribs is determined. Third, the grouping scheme of the ribs is determined according to the results of the topology optimization. Finally, parametric optimization is applied to determine the final optimized structure of the mirror. Compared with the conventional lightweight design method, this method has significant advantages: (1) compared with topology optimization based on a continuum solid blank, the cost of computation can be greatly reduced using a mirror of linear discrete shell elements; (2) this method avoids the blind grouping of lightweight ribs; and (3) this method fully combines the advantages of topology optimization and parametric optimization.

In this study, an optimal lightweight design for a 676-mm-outer-diameter SiC primary mirror derived using a topology- and parametric-based optimization method is presented. In Sec. 2, the requirements of a space reflective mirror and theory on both topology optimization and parametric optimization are introduced. In Sec. 3, a detailed lightweight design of the space reflective mirror using the topology- and parametric-based optimization method is carried out, and the performance of the optimum mirror is compared with the initial design. The conclusions are given in Sec. 4.

2 Topology and Parametric Optimization Based Design Method

2.1 *Requirements of a Space Reflective Mirror*

In this paper, a parametric optimization method for large-space mirrors based on topology optimization of the basic configuration is used to design an optimal lightweight structure. Typically, space mirrors are manufactured and tested on the ground, and then launched into space. Since the space is a microgravity environment, the effect of gravity release on the mirror may affect its optical performance. Therefore, it is necessary that the surface shape of the mirror is maintained to high precision under a range of load conditions. In addition, to prevent the mirror from vibration damage during the launch, it is very important to ensure its good dynamic stiffness.

The surface shape error is generally described in one of two ways:[13] the peak value of the mirror surface deformation minus the valley value, also called the PV value, or the RMS value of the mirror surface shape error, which is the RMS of the normal displacement without the rigid body displacement:

$$\mathrm{PV} = \max\{U_1^n, U_2^n, \ldots, U_N^n\} - \min\{U_1^n, U_2^n, \ldots \infty, U_N^n\}, \tag{1}$$

$$\mathrm{RMS} = \sqrt{\sum_i^N w_i R_i^2}, \tag{2}$$

where $R_i = U_i^n - Z_{i1} - Z_{i2} - Z_{i3}$; N is the total number of the nodes on the mirror surface; w_i is the weight factor of the i'th node; and Z_{i1}, Z_{i2}, and Z_{i3} are the lower-order terms of the Zernike polynomials, which represent the piston, tilt, and defocus of the mirror face, respectively. Given that the mirror face is discretized by finite-element method in the calculation process and U_i^n is the normal displacement of the i'th node, which contains both the direction and magnitude. However, it is very difficult to directly set the surface RMS value as the objective merit function of a topology optimization model. In addition, for high-precision optical surfaces, there are multiple relationships between the PV value and the RMS value.[14] Therefore, to improve the computational efficiency, the upper limit of the PV value is selected as the design constraint in the topology optimization model, and the RMS value is used as the objective merit function to establish the parametric optimization model.

2.2 *Topology Optimization Model*

The variable density method is a commonly used continuum topology optimization method. The basic idea is to introduce a kind of hypothetical material with variable density, and the material density is set as the design variable in the topology optimization problem, so that the structural topology optimization problem is transformed into a problem of the optimal distribution of the material. The solid isotropic microstructure with penalization (SIMP) model is a commonly used interpolation model in the variable density method.[15,16] According to the idea of continuum structure topology optimization, the finite-element model is established with linear shell elements. A description factor, ρ, is introduced for each element. Whether there is material in each element or not is determined by the ρ value of 1 or 0. In addition, intermediate

density values are penalized by a penalty factor, and the intermediate density values are then clustered at both ends of the 0 to 1 range, so that the topology optimization model of the continuous variable can converge well to the optimization model:

$$E_i = (\rho_i)^r E_0, \quad V_i^s = \rho_i V_i, \qquad i = 1, 2, \ldots, n. \tag{3}$$

Here, n is the total number of the discrete finite elements; ρ_i, E_i, and V_i^s are the description factor, material elastic modulus, and the volume of the solid material of the i'th element, respectively. E_0 is the elastic modulus of a given material, V_i is the volume of the i'th element, and r is the penalty factor. Thus, the problem of mirror structural design is transformed into a problem to find a combination of material factors for each element. Therefore, the design variable can be expressed as follows:

$$X = (\rho_1, \rho_2, \ldots, \rho_n)^T. \tag{4}$$

The goal of the topology optimization is to minimize the amount of material while maintaining the optical performance of the mirror. The objective merit function can be expressed as follows:

$$f(X) = \sum_{i=1}^{n} \rho_i V_i. \tag{5}$$

To facilitate manufacturing and testing, space mirrors are usually designed in a centrally symmetric form. Therefore, to ensure that the structure of the optimized mirror has a symmetric configuration, a pattern repetition constraint is imposed on the topology optimization problem. This constraint can be expressed as follows:

$$G_k(X) = 0, \tag{6}$$

where $G_k(X)$ represents the symmetric constraint between the k'th elements.

The topology optimization mathematical model of the mirror can then be expressed as follows:

$$\begin{aligned}
&\text{Find} \qquad X = (\rho_1, \rho_2, \ldots, \rho_n)^{\mathrm{T}} \\
&\text{Minimize} \qquad f(X) = \sum_{i=1}^{n} \rho_i V_i \\
&\text{Subject to} \\
&\mathrm{PV} = \max\{U_1^n, U_2^n, \ldots, U_N^n\} - \min\{U_1^n, U_2^n, \ldots, U_N^n\} \le \overline{U} \\
&G_k(X) = 0 \\
&0 < \rho_{\min} \le \rho_i \le 1,
\end{aligned} \tag{7}$$

where $\overline{U}$ is the upper limit of the PV value of the mirror surface shape error and $\rho_{\min}$ is the lower bound of the description factor, which is introduced to avoid the singularity of the stiffness matrix in the optimization process.

2.3 *Parametric Optimization Model*

For web-skin-type space mirrors, the results of the topology optimization will give a different material distribution for each stiffener (rib). Therefore, the ribs can be easily grouped based on the topology optimization results. Lightweight ribs with similar material distributions are taken as a set of design variables in the parametric optimization model. After grouping the ribs according to the topology optimization results, further optimization is needed to determine the final dimensions of each group of ribs. However, the number of ribs is usually very large, and if all the ribs of the group are individually set as design parameters, the computation time will be significant. Additionally, too many structural parameters will cause manufacturing difficulties. Therefore, it is necessary to identify the key factors that affect the objective merit function significantly before carrying out the optimization. The design of experiment (DoE) method is a statistical method that can be used to effectively understand the effects of multiple factors on the output by determining which are statistically significant.[17,18] In general, the DoE results usually provide an approximate model between the input factors X_i and the output response Y in the form of a lower-order polynomial, such as

$$Y = C_0 + \sum_{i=1}^{m} C_i X_i + \sum_{i=1,j=1}^{m} C_{ij} X_i X_j. \tag{8}$$

The magnitudes of the coefficients in this equation reflect the strength of the effects of factors X_i on the model output response Y. As a result, the contributions of the absolute values of the input factor coefficients can be determined and the key factors identified. Commonly used DoE algorithms include the parameter study method, full factorial design, central composite design, the orthogonal array method, and the Latin hypercube design method. Generally, the more sample points are used, the more accurate the analysis results obtained are. However, considering the computation expense in practical problems, as few samples as possible are usually selected to design the test while maintaining the accuracy of the results.

According to the results of the sensitivity analysis obtained by DoE, the key factors are chosen as design variables used in the parametric optimization model, which are expressed as follows:

$$P = (p_1, p_2, \ldots, p_s)^{\mathrm{T}}, \tag{9}$$

where p_i is the i'th design parameter and s is the total number of the design parameters. The mathematical model of parametric optimization is established as follows:

$$\begin{aligned}
&\text{Find} \qquad P = (p_1, p_2, \ldots, p_s)^{\mathrm{T}} \\
&\text{Minimize} \\
&\quad \mathrm{RMS}, \\
&\quad \mathrm{Mass}. \\
&\text{Subject to} \\
&\quad \mathrm{RMS} \le \delta, \\
&\quad \mathrm{Mass} \le \overline{\mathrm{Mass}}. \\
&\quad f_1 \ge \mathit{f}, \\
&\quad p_{i,\mathrm{low}} \le p_i \le p_{i,\mathrm{up}}, \qquad i = 1, 2, \ldots, s,
\end{aligned} \tag{10}$$

where RMS is the RMS value of the surface shape error of the mirror under certain load condition; δ is the upper limit of

the RMS value; Mass is the mass of the mirror; $\overline{\text{Mass}}$ is the maximum limit of the mass; f_1 is the first-order natural frequency, with f as its lower limit; and $p_{i,\text{low}}$ and $p_{i,\text{up}}$ are the lower and upper limits of p_i, respectively.

In this paper, the computer-aided drafting model was imported into the OptiStruct tool of HyperWorks to perform the topology of the mirror. The deformation of the mirror surface was calculated through OptiStruct, and then the nodal displacement from the finite-element analysis was evaluated by MATLAB codes. The sensitivity analysis and parametric optimization were performed by means of Isight software, which integrated the OptiStruct and MATLAB software. The computer used in the topology and parametric optimization was a Dell workstation configured with two Intel Xeon E5-2687w CPUs and 64 GB memory.

3 Lightweight Design of the Space Reflective Mirror

3.1 *Initial Design of the Mirror*

Some researchers have carried out performance comparisons for lightweight mirrors with differently shaped honeycomb holes to identify those structures with better comprehensive performance.[19,20] The most commonly used polygon core configurations include triangular, square, and hexagonal. Compared to the square and hexagonal configurations, the triangular configuration shows better optical performance, higher stiffness, and good workability while maintaining the same geometry. In this paper, we use triangular polygon core configurations as the initial design. Figure 1(a) presents the initial design of the space reflective mirror. The outer ring diameter is 676 mm, the clear aperture is 660 mm, and the inner ring diameter is 567 mm. The thickness of the mirror face is 5 mm. The initial thickness of the lightweight ribs is uniformly taken as 4 mm, and the inner and outer ring thicknesses as 6 and 4 mm, respectively. The mirror is supported by three points on its back. The distance between the center of the support hole and the center of the mirror is 208 mm. To support the mirror laterally, radial ribs were used at the outer beveled rim of the reflective mirror. Table 1 lists the initial dimensions of the mirror. In this paper, we chose SiC as our mirror material, which has the following key properties: Young's modulus = 330 GPa, density = 3.20 g/cm^3, and Poissonn's ratio = 0.18. The total mass of the solid space reflective mirror excluding lightweight cells in the rear face is 93.12 kg. Accordingly, the mass of the initial reflective mirror was 20.40 kg and a 78.0% lightweight ratio was achieved. Figure 1(b) shows a three-dimensional geometry model of the initial lightweight design of the mirror.

According to the design requirements for structural static stiffness, the RMS values of the surface shape error of the mirror parallel to the X, Y, and Z axes under gravity should be no more than $\lambda/50$, $\lambda/70$, and $\lambda/70$ (where $\lambda = 632.8$ nm represents the wavelength of visible light). In addition, to prevent the mirror from vibration damage during the launch, the first-order natural frequency of the mirror must not be less than 1000 Hz. Furthermore, to reduce launch costs, the mass of the mirror should be less than 25.0 kg.

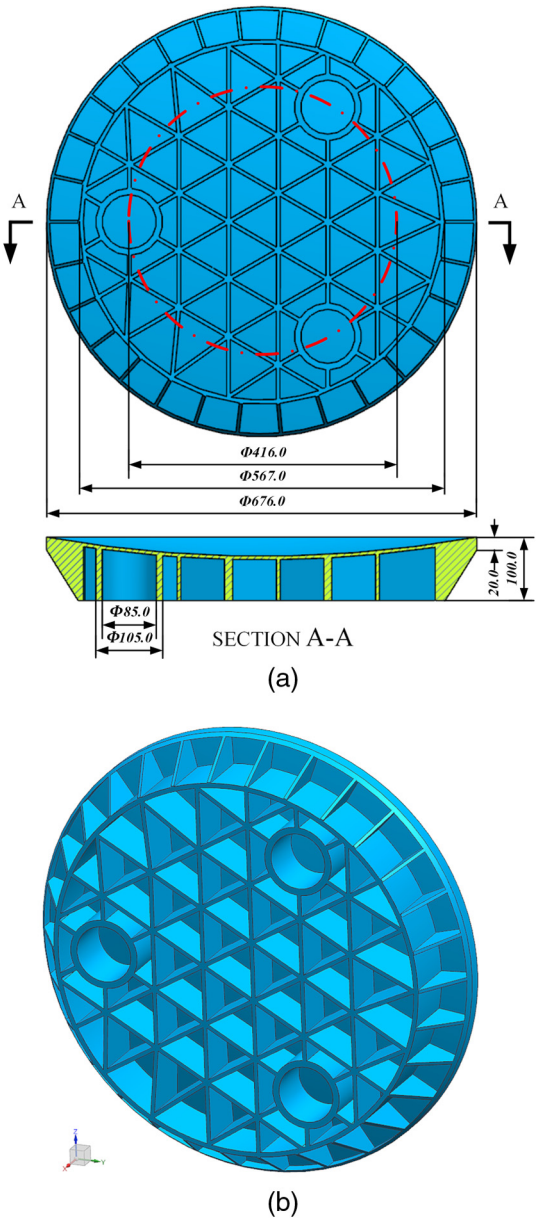

Fig. 1 Initial lightweight design of the space reflective mirror: (a) basic dimensions and (b) solid model.

3.2 *Topology Optimization of the Mirror*

The mirror discussed in this paper is a web-skin-type mirror. To improve the optimization efficiency and reduce the computational cost of the topology optimization, the finite-element model is established with linear shell elements. The total number of nodes is 7713, and the total number of elements is 8201. To obtain accurate result, the mapped mesh was applied to the mirror surface. In general, the deformation of the reflector is most serious when the direction of gravity is parallel to the optical axis. Therefore, the upper limit of the displacement (20 nm) of the node on the face of the mirror in the optical axis direction is taken as the constraint, and the total mass of the mirror is set as the objective.

The topology optimization model comprises a design domain and a nondesign domain. The three support holes, the mirror face, the inner ring, and the outer ring are assigned to the nondesign domain and all the ribs to the design

Table 1 Initial dimensions of the lightweight space reflective mirror.

Components	Value
Outer ring diameter	676.0 mm
Inner ring diameter	567.0 mm
Rib thickness	4.0 mm
Outer ring thickness	4.0 mm
Inner ring thickness	6.0 mm
Thickness at the outer ring rim	20.0 mm
Thickness at the inner ring rim	100.0 mm
Total mass	20.40 kg
Lightweight ratio	78.0%

domain. In addition, to generate a central symmetric configuration, a pattern repetition constraint is imposed in the design domain. The response fully converges to minimum values after 145 iterations. Figure 2 shows the material distribution results of the topology optimization. The red part represents elements with a density of 1, and the blue part represents elements with a density close to zero. Accordingly, the ribs can be easily grouped based on the topology optimization results. Figure 3 shows the ribs grouped in this way.

3.3 *Parametric Optimization of the Mirror*

For better manufacturing and testing, the mirror is usually designed as a centrally symmetric structure, and the lightweight ribs distributed on the back of the mirror have a distinct geometric distribution. Thus, the ribs can be grouped according to their geometric position characteristics. Figures 4 and 5 show the schematic models of the conventional design and the ribs grouped according to their geometric position characteristics, respectively.

Due to the fabrication limit of our optical shop, the initial thicknesses of the ribs are set to 4 mm, and a range of 3 to 8 mm is used for the variation of the rib thickness. The rest of the dimensions are maintained at the initial design value. For a large SiC mirror supported by three holes located on the back of the mirror, the deformation of the mirror face is worst when the gravity is parallel to the optical axis. To examine how ribs of different thicknesses contribute to the quality of the optical surface, the RMS value of the mirror for gravity parallel to the optical axis is taken as the objective merit function. Table 2 shows the optimization results of the following three schemes: no grouping of the ribs, grouping of the ribs based on geometry, and grouping of the ribs based on topology optimization. According to Table 2, the masses of the mirrors obtained using the three schemes are 28.12, 24.34, and 21.44 kg, and the RMS values of the surface shape error of the mirrors are 18.74, 16.98, and 15.30 nm, respectively. From Table 2, we can see that the thicknesses of the ribs vary a lot when the ribs are grouped based on topology optimization results. The thickness of the thickest ribs is 7.96 mm, and these are mainly concentrated in the vicinity of the three support holes, while the thickness of the thinnest ribs is only 3.03 mm. The maximum difference in thickness between the thickest ribs and the thinnest ribs is almost 5 mm. In addition, compared with the traditional design, the quality of the optical surface obtained by ribs grouped based on the results of topology optimization and geometric characteristics is improved by about 18.36% and 9.3%, respectively, and the mass of the mirror is reduced by 23.76% and 13.44%, respectively.

This result shows that, compared with the traditional design, these two improved designs can significantly

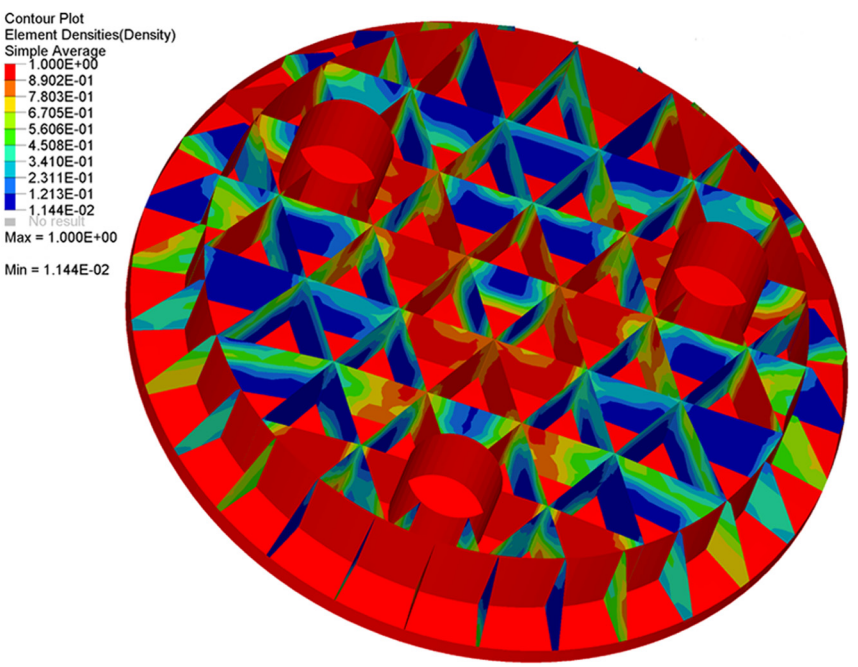

Fig. 2 Material distribution result of the topology optimization. The red part represents elements with a density of 1, and the blue part represents elements with a density close to zero.

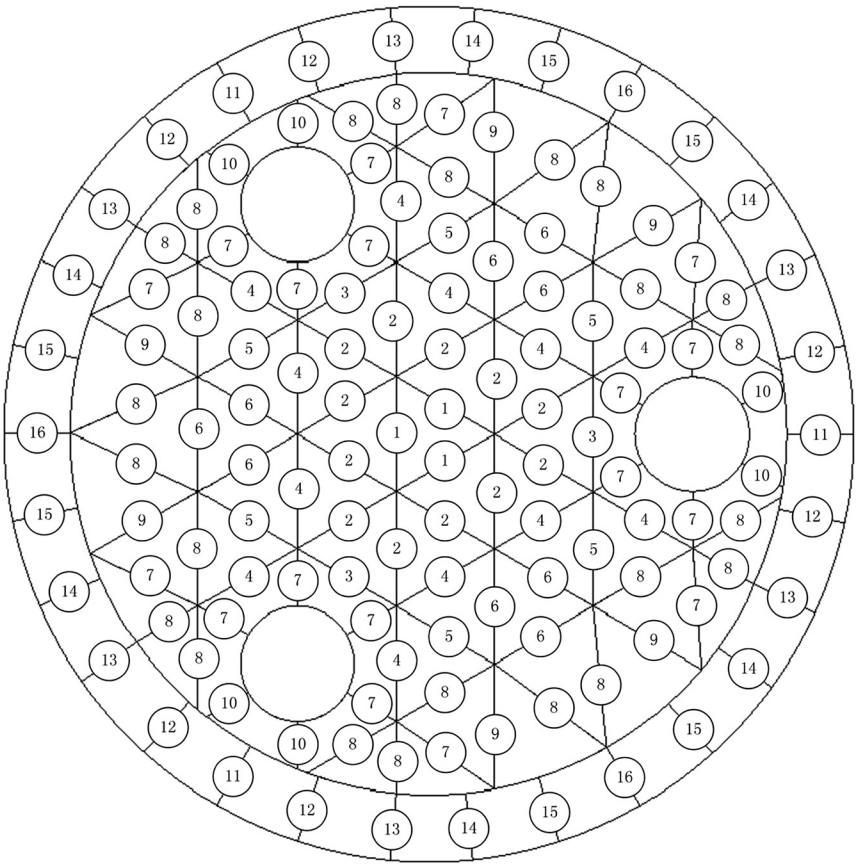

Fig. 3 Lightweight ribs grouped according to the topology optimization results.

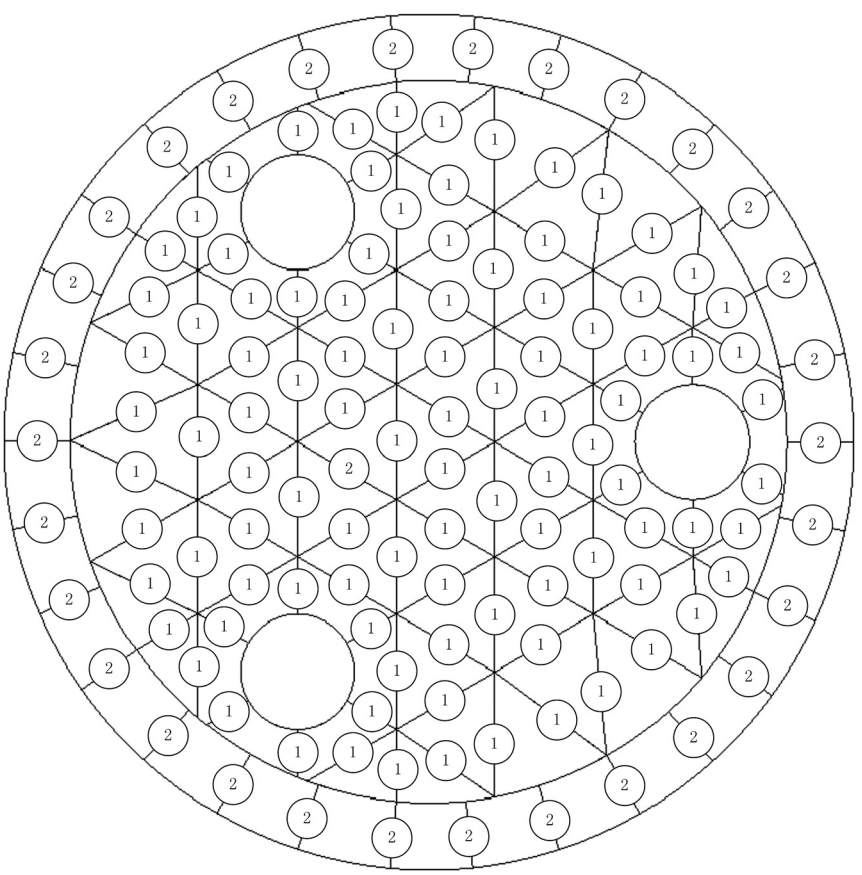

Fig. 4 Grouping of the ribs for the traditional design.

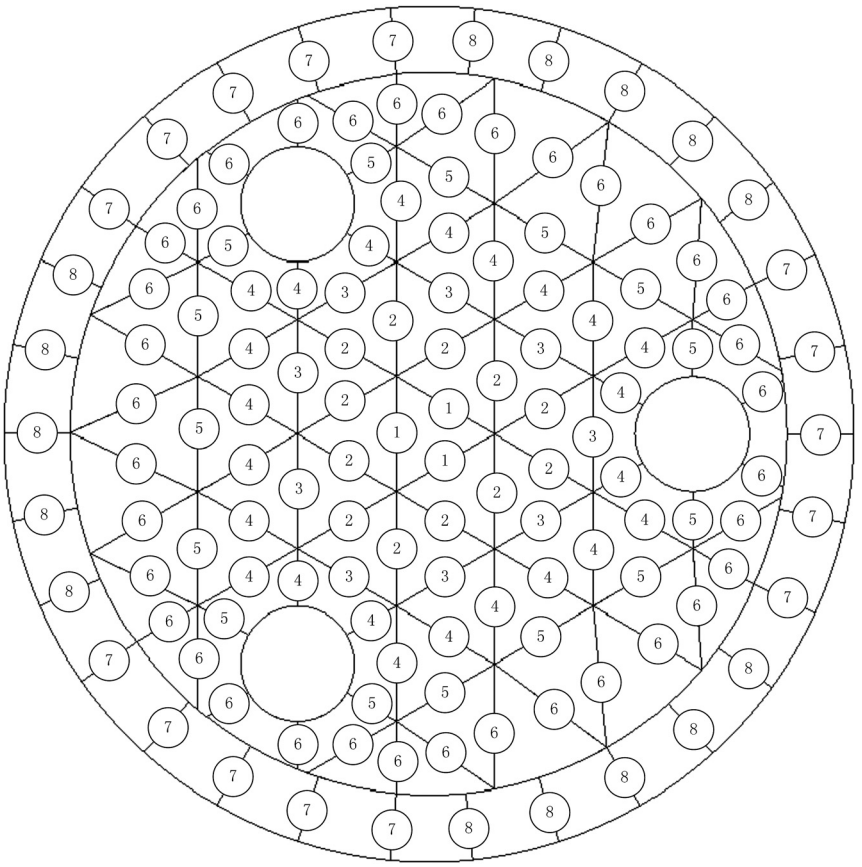

Fig. 5 Grouping of the ribs according to the geometric position characteristics.

improve the quality of the optical surface of the mirror while reducing its mass. Moreover, the optimal mirror based on ribs grouped by topology optimization shows significant advantages, with a lower mirror mass and a higher optical surface quality. There are two main reasons for this: (1) the local stiffness of the mirror is strongly affected by the structure parameters at the corresponding location. For a given load condition, not all ribs contribute equally. Therefore, it is possible to improve the quality of the optical surface of the mirror by adjusting the thicknesses of the lightweight ribs at different positions. (2) Although these two schemes are carried out based on different methods, this method increases the degree of freedom of the design and expands the solution space of the design problem, giving better optimum results.

Based on this analysis, it can be seen that the thicknesses of the lightweight ribs at different positions on the mirror have a significant influence on the quality of the optical surface. However, the results obtained from grouping schemes mentioned above do not meet the design requirements. Therefore, the structural parameters of the mirror need to be further optimized. In fact, in the actual optimization process, the shape optimization of the structure tends to be more efficient than the size optimization at improving the optical performance of the mirror. Considering that the influence of the structural parameters on the optical surface quality cannot be simply superimposed, the parameters are coupled with each other, so that the solution space of the optimal design problem is very complex. Combined with the previous analysis results, and considering the other structure parameters (such as the mirror face thickness and the diameter of the supporting hole), the lightweight mirror structure is characterized by 26 parameters, as shown in Fig. 6. Outer ring thickness is described by parameter 19, and inner ring thicknesses are described by parameter 20 (far away from the support holes) and parameter 21 (near the support holes). Thicknesses at the outer and inner ring rim are described by parameter 24 and parameter 25, respectively. The middiameter of support hole is described by parameter 26, and parameter 22 represents the thickness of the support hole.

4 Design of Experiment and Integrated Optimization

The orthogonal arrays method is used to design the experiment for the parameters of the lightweight space mirror. There are a total of 26 factors, that is, the 26 parameters of the lightweight mirror structure, as shown in Fig. 6. Each factor contains two levels. Given the computational expense and the accuracy required, an orthogonal table, $L_{64}(2^{63})$, is used. As mentioned earlier, in the structural design of the space mirror, it is necessary to maintain the high precision of the surface shape error of the mirror under multiple load conditions and high dynamic stiffness while reducing the mass of the mirror as far as possible. Therefore, the response of the DoE is selected according to these three aspects. However, due to the differences of each response in terms of relative importance, magnitude, and dimensions, it is very difficult to determine each weight factor if the responses are weighted uniformly through linear

Table 2 Optimal thicknesses of the lightweight ribs, the mirror masses, and the RMS values for the three different schemes.

Design variables	Without grouping	Grouped based on geometry	Grouped based on topology optimization
Ribs1 (mm)	7.80	3.19	4.50
Ribs2 (mm)	3.01	3.52	4.61
Ribs3 (mm)	—	7.42	7.42
Ribs4 (mm)	—	7.99	3.54
Ribs5 (mm)	—	7.64	7.37
Ribs6 (mm)	—	3.85	3.24
Ribs7 (mm)	—	6.35	7.96
Ribs8 (mm)	—	3.34	3.04
Ribs9 (mm)	—	—	3.03
Ribs10 (mm)	—	—	3.26
Ribs11 (mm)	—	—	7.73
Ribs12 (mm)	—	—	5.19
Ribs13 (mm)	—	—	3.40
Ribs14 (mm)	—	—	3.18
Ribs15 (mm)	—	—	3.60
Ribs16 (mm)	—	—	3.34
		Response	
Mass (kg)	28.12	24.34	21.44
RMS (nm)	18.74	16.98	15.30

combination. In addition, there are a lot of algorithms available in the literature for multiobjective optimization problems (MOPs), such as the nondominated sorting genetic algorithm (NSGA) and its second generation (NSGA-II), the neighborhood cultivation genetic algorithm, and the archive-based micro genetic algorithm.[21–24] Therefore, the above three aspects of the response are defined as follows: response 1: OEI, which is the overall environmental impact on the RMS value of the surface shape error of the mirror; response 2: Mass; and response 3: f_1. The definition of the OEI is as follows:

$$\mathrm{OEI} = w_1\mathrm{RMS}_{\mathrm{G\text{-}}X} + w_2\mathrm{RMS}_{\mathrm{G\text{-}}Y} + w_3\mathrm{RMS}_{\mathrm{G\text{-}}Z}, \tag{11}$$

where $\mathrm{RMS}_{\mathrm{G\text{-}}X}$, $\mathrm{RMS}_{\mathrm{G\text{-}}Y}$, and $\mathrm{RMS}_{\mathrm{G\text{-}}Z}$ represent the RMS values of the surface shape error of the mirror under gravity parallel to the X, Y, and Z axes, respectively. Considering the differences in the deformation of the mirror under gravity parallel to the optical axis and perpendicular to the optical axis, the corresponding weight factors were set to 0.5, 0.25, and 0.25, respectively.

Figure 7 shows a flowchart of the entire DoE. Following the analysis results for the sample data, the linear regression model between the factors and the three responses is established. In the linear regression model, the magnitudes of the coefficients of each term represent the degree to which the factor contributes to the response. In other words, the coefficient represents the sensitivity of the corresponding input parameter (design variable) to the response. Figure 8 shows the normalized percentage of the contributions of the input factors to the three responses, which also reflects the sensitivities of the responses to the input factors.

Based on the results of the sensitivity analysis, p_8, p_9, p_{11}, p_{17}, p_{19}, p_{20}, p_{21}, p_{22}, p_{23}, p_{24}, p_{25}, and p_{26}, which have greater contributions to the three responses, are the key parameters. Subsequently, these parameters are selected as the design variables for the size and shape optimization process, expressed as follows:

$$P = (p_8, p_9, p_{11}, p_{17}, p_{19}, p_{20}, p_{21}, p_{22}, p_{23}, p_{24}, p_{25}, p_{26})^{\mathrm{T}}. \tag{12}$$

The first-order natural frequency, f_1, which is usually easier to use to satisfy the design requirements, is selected as the constraint. Therefore, the size and shape optimization process of the lightweight mirror can be summarized as follows:

$$\begin{aligned}
&\text{Find} \quad P = (p_1, p_2, \ldots, p_s)^{\mathrm{T}} \\
&\text{Minimize} \\
&\qquad \mathrm{OEI} = \mathrm{OEI}(P), \\
&\qquad \mathrm{Mass} = \mathrm{Mass}(P). \\
&\text{Subject to} \\
&\qquad \mathrm{RMS}_{\mathrm{G\text{-}}X} \le \delta_1, \\
&\qquad \mathrm{RMS}_{\mathrm{G\text{-}}Y} \le \delta_2, \\
&\qquad \mathrm{RMS}_{\mathrm{G\text{-}}Z} \le \delta_3, \\
&\qquad \mathrm{Mass} \le \overline{\mathrm{Mass}}. \\
&\qquad f_1 \ge \underline{f}, \\
&\qquad p_{i,\mathrm{low}} \le p_i \le p_{i,\mathrm{up}}, \qquad i = 1, 2, \ldots, s,
\end{aligned} \tag{13}$$

where δ_1, δ_2, and δ_3 are the upper limits of the values of $\mathrm{RMS}_{\mathrm{G\text{-}}X}$, $\mathrm{RMS}_{\mathrm{G\text{-}}Y}$, and $\mathrm{RMS}_{\mathrm{G\text{-}}Z}$, respectively.

5 Results and Discussion

Nonlinear MOPs are always concerned with several (often conflicting) objective functions that must be optimized simultaneously. However, in general, a solution that is simultaneously optimal for all of the objectives is not feasible, and the real purpose of multiobjective optimization is to identify the set of so-called Pareto-optimal solutions.[25] This set of solutions represents the best options available.

Figure 9 shows the optimization result obtained using the NSGA-II routine. The axes are the performance metrics, which are the mirror mass and the OEI. Over 4000 designs were evaluated, and the time spent in performing the parametric optimization was 8 h. Based on the Pareto front illustrated in Fig. 9, we can see that these two performance metrics are inversely proportional in reaching the design goal. After obtaining the set of Pareto-optimal solutions, we select one of the solutions considering the RMS value

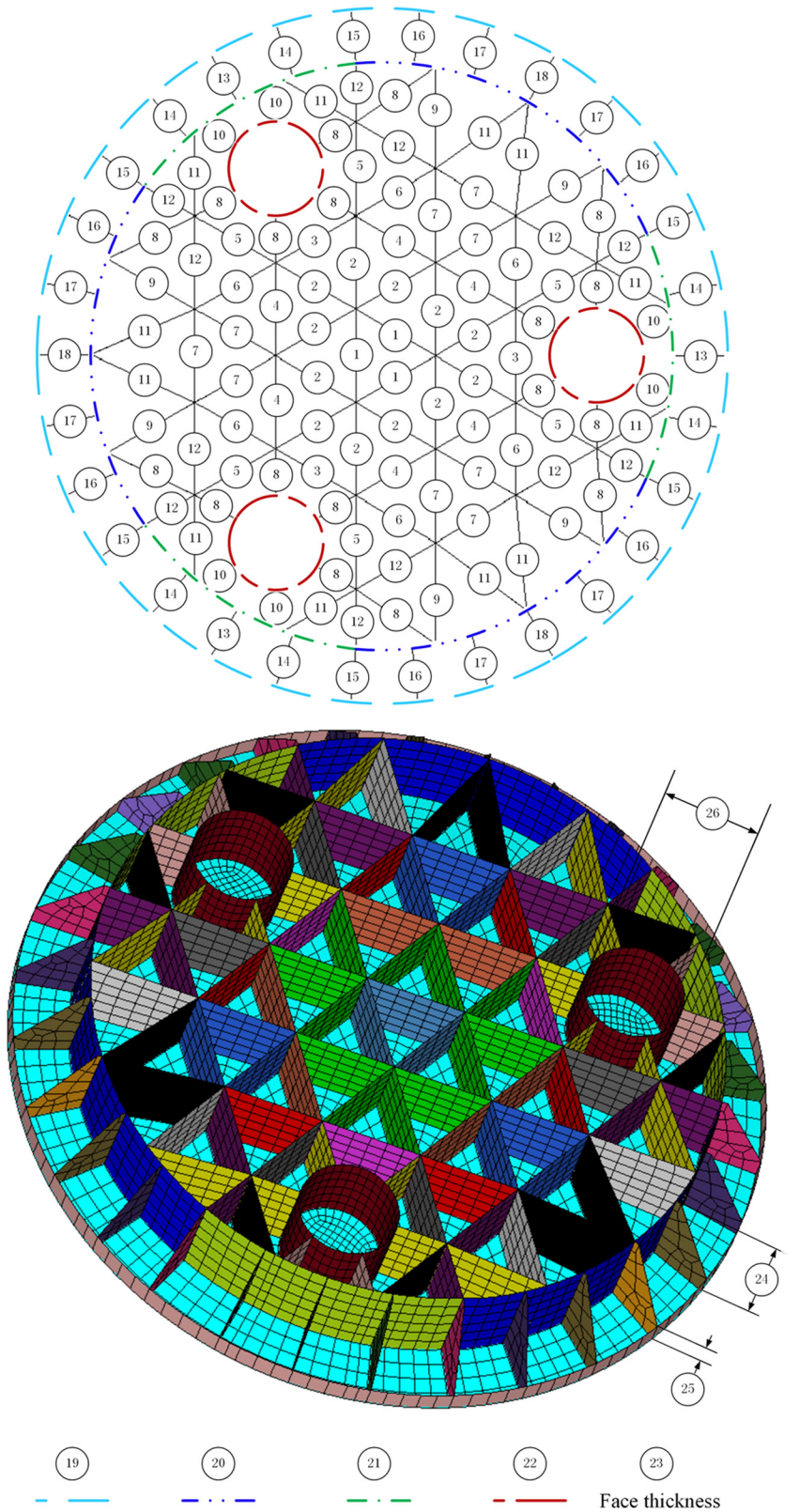

Fig. 6 Schematic diagram of the structure parameters of the mirror and its finite-element model.

of the surface shape error of the mirror and the total mass of the mirror. The upper bound, lower bound, initial values, and optimum values of the design parameters are listed in Table 3. According to Table 3, the optimum values of p_9, p_{11}, and p_{17}, which represent the thicknesses of the ribs, were lower than their respective initial values; however, p_8 was increased from its initial value of 4.00 mm to an optimum value of 7.91 mm. The optimum values of p_9 and p_{11} have almost reached their respective lower bounds. By contrast, the optimum values of p_8, p_{21}, p_{24}, and p_{26} have

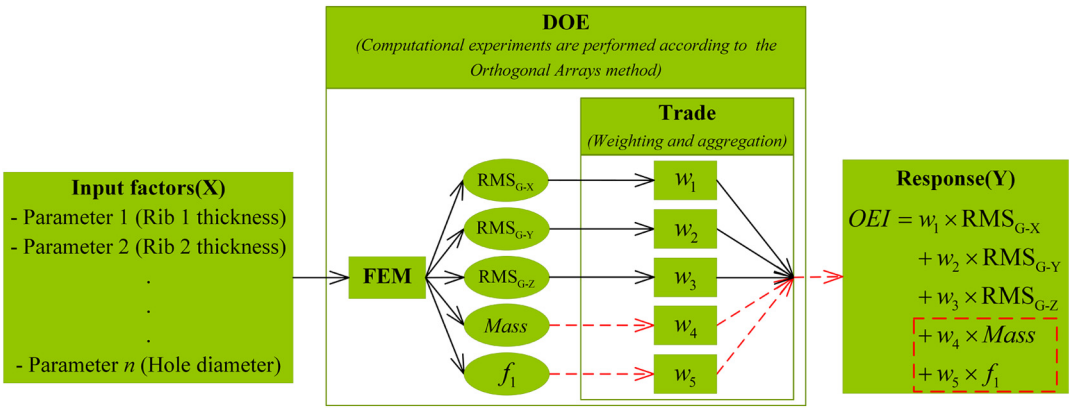

Fig. 7 Schematic diagram showing the design of the experiment based on the orthogonal arrays method.

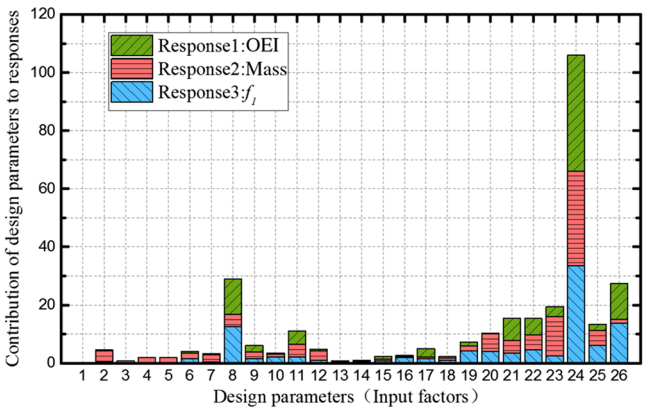

Fig. 8 Contributions of the design parameters to the responses.

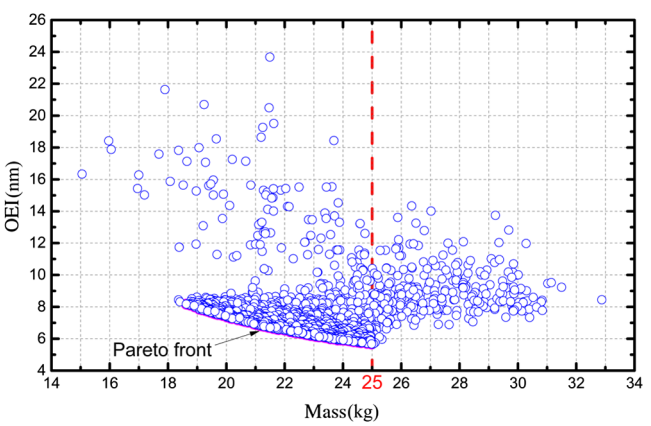

Fig. 9 Design optimization results for the lightweight mirror.

almost reached their respective upper bounds. The thickness of the inner ring is characterized by two parameters, p_{20} and p_{21}, both of which were set to 6.00 mm in the initial design. The optimal values of p_{20} and p_{21} are 3.85 and 9.46 mm, with the difference reaching 4.6 mm. Thus, not all ribs contribute to the load distribution. In addition, the variations in p_{24}, p_{25}, and p_{26} are much greater than those for the other design parameters. Among these, the value of p_{25}, which represents the thickness at the outer ring rim, decreased from 20.00 to 5.52 mm, and the values of p_{24} and p_{26} were increased by 24.31 and 17.98 mm, respectively.

Table 3 Upper bound, lower bound, initial values, and optimum values of the design parameters.

Design parameter	Lower bound (mm)	Upper bound (mm)	Initial value (mm)	Optimum value (mm)
p_8	3.00	8.00	4.00	7.91
p_9	3.00	8.00	4.00	3.05
p_{11}	3.00	8.00	4.00	3.06
p_{17}	3.00	8.00	4.00	3.11
p_{19}	3.00	10.00	4.00	3.45
p_{20}	3.00	10.00	6.00	3.86
p_{21}	3.00	10.00	6.00	9.46
p_{22}	6.00	14.00	10.00	12.52
p_{23}	4.00	8.00	5.00	4.01
p_{24}	75.00	125.00	100.00	124.31
p_{25}	5.00	35.00	20.00	5.52
p_{26}	72.00	108.00	90.00	107.98

The normal deformation contour of the mirror face after optimization is shown in Fig. 10. Table 4 shows a comparison of the responses between the initial design and the optimum design. According to Table 4, the overall environmental impact on the RMS value of the surface shape error of the mirror decreased from 11.34 to 5.42 nm. For gravity vertical to the optical axis, the RMS values of the initial and optimal designs are no more than 3 nm. However, for gravity parallel to the optical axis, the RMS value for the optimal mirror is 8.44 nm, and the RMS value of the initial design is 19.92 nm. Based on this result, we can conclude that the RMS difference between the initial and optimal designs under gravity vertical to the optical axis is not obvious, whereas for gravity parallel to the optical axis, the optimal design has almost an 11.5 nm improvement in the RMS value, and the quality of the optical surface is improved by more than 57.6%. The first-order natural frequency of the optimal mirror is 2393.4 Hz, which is about 30.2% higher

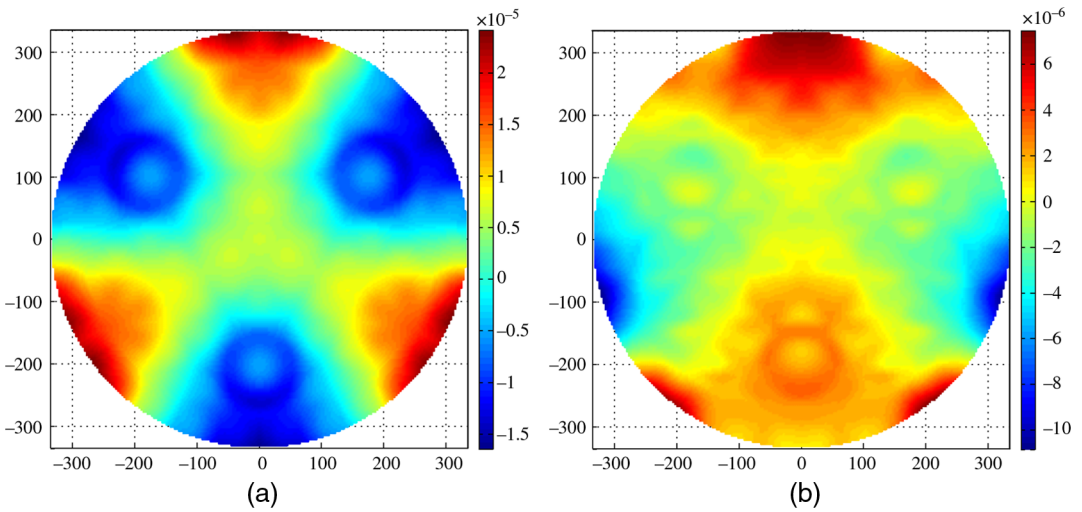

Fig. 10 Normal displacement contour of the mirror face: (a) gravity parallel to the optical axis and (b) gravity vertical to the optical axis.

Table 4 Comparison of responses between the initial and optimum designs.

Responses	OEI (nm)	$RMS_{G\text{-}X}$ (nm)	$RMS_{G\text{-}Y}$ (nm)	$RMS_{G\text{-}Z}$ (nm)	Mass (kg)	f_1 (Hz)
Initial value	11.34	19.92	2.76	2.77	20.40	1838.2
Optimum value	5.42	8.44	2.39	2.39	24.98	2393.4

than that of the initial design. In addition, the optimized reflector quality increased substantially, while the weight increased only slightly. As can be seen from the results presented in Tables 3 and 4, the shape changes improve the optical performance of the lightweight mirror more effectively than the size changes.

6 Conclusions

In this paper, a parametric optimization method to design large, lightweight space mirrors based on topology optimization of the basic mirror configuration has been proposed. This method combines the advantages of topology optimization and parametric optimization, and the optimal material distribution obtained from topology optimization is used as the basis for grouping the lightweight ribs. The optimization result for the ribs shows that the local stiffness of the mirror is significantly affected by the structure parameters at the corresponding locations. Not all ribs contribute equally for a given load condition. The integrated optimization of the mirrors shows that shape optimization improves the optical performance of lightweight mirrors more effectively than size optimization of the structure parameters. Compared with the initial design, the quality of the optical surface of the optimized mirror with gravity parallel to the optical axis is improved by more than 57.6%, and the first-order natural frequency of the mirror is increased by 30.2%. These results demonstrate the effectiveness of the space mirror optimization design method proposed in this paper.

Acknowledgments

This work was supported by the National Natural Science Foundation of China (Grant No. 61605203) and the Youth Innovation Promotion Association of the Chinese Academy of Sciences (Grant No. 2015173). We thank Liwen Bianji, Edanz Editing China (www.liwenbianji.cn/ac), for editing the English text of a draft of this manuscript.

References

1. L. E. Cohan and D. W. Miller, "Integrated modeling for design of lightweight, active mirrors," *Opt. Eng.* **50**, 063003 (2011).
2. N. Ebizuka et al., "Development of SiC ultra light mirror for large space telescope and for extremely huge ground-based telescope," *Proc. SPIE* **4842**, 329–334 (2003).
3. Y. Zhang et al., "Large-scale fabrication of lightweight Si/SiC ceramic composite optical mirror," *Mater. Lett.* **58**, 1204–1208 (2004).
4. R. Sahu et al., "Structural optimization of a space mirror to selectively constrain optical aberrations," *Struct. Multidiscip. Optim.* **55**(6), 2353–2363 (2017).
5. K. S. Park, S. Y. Chang, and S. K. Youn, "Topology optimization of the primary mirror of a multi-spectral camera," *Struct. Multidiscip. Optim.* **25**(1), 46–53 (2003).
6. K. S. Park, J. H. Lee, and S. K. Youn, "Lightweight mirror design method using topology optimization," *Opt. Eng.* **44**, 053002 (2005).
7. S. Liu et al., "Topology optimization-based lightweight primary mirror design of a large-aperture space telescope," *Appl. Opt.* **53**, 8318–8325 (2014).
8. Y. C. Chen et al., "Optimization of lightweight structure and supporting bipod flexure for a space mirror," *Appl. Opt.* **55**, 10382–10391 (2016).
9. H. Kihm and H. S. Yang, "Design optimization of a 1-m lightweight mirror for a space telescope," *Opt. Eng.* **52**, 091806 (2013).
10. H. Kihm et al., "1-m lightweight mirror design using genetic algorithm," *Proc. SPIE* **8415**, 841514 (2012).
11. J. Yuan and J. Y. Ren, "Improvement and optimization of lightweight structure for SiC reflective mirror," *Acta Photonica Sin.* **44**, 34–39 (2015).
12. W. Zhang and Y. Yang, "Design of lightweight mirror based on genetic algorithm," *Proc. SPIE* **6148**, 61480T (2006).
13. V. N. Mahajan, "Zernike circle polynomials and optical aberrations of systems with circular pupils," *Appl. Opt.* **33**, 8121–8124 (1994).
14. M. Bayar, *Optomechanical Systems Design*, Marcel Dekker, New York (1986).
15. M. P. Bendsøe and O. Sigmund, "Material interpolation schemes in topology optimization," *Arch. Appl. Mech.* **69**, 635–654 (1999).
16. S. Amstutz, "Connections between topological sensitivity analysis and material interpolation schemes in topology optimization," *Struct. Multidiscip. Optim.* **43**, 755–765 (2011).
17. M. Anderson and P. Whitcomb, "Design of experiments: statistical principles of research design and analysis," *Technometrics* **43**, 236–237 (2001).
18. R. A. Fisher, "The design of experiments," *Int. J. Plant Sci.* **57**, 183–189 (1935).

19. D. Vukobratovich, "A comparison of the merits of open-back, symmetric sandwich, and contoured back mirrors as light-weighted optics," *Proc. SPIE* **1167**, 20–36 (1989).
20. M. A. Abdulkadyrov et al., "Optimizing design and manufacturability of reduced-weight mirrors for astronomy and space applications," *J. Opt. Technol.* **83**, 168–172 (2016).
21. K. Deb et al., "A fast and elitist multiobjective genetic algorithm: NSGA-II," *IEEE Trans. Evol. Comput.* **6**, 182–197 (2002).
22. C. M. Fonseca and P. J. Fleming, "An overview of evolutionary algorithms in multiobjective optimization," *Evol. Comput.* **3**, 1–16 (1995).
23. C. M. Fonseca and P. J. Fleming, "Genetic algorithms for multiobjective optimization: formulation, discussion, generalization," in *Proc. of the 5th Int. Conf. on Genetic Algorithms*, pp. 416–423 (1993).
24. L. I. Cheng-Hong, H. E. Ying, and X. A. University, "The NSGA- II application optimization allocation of water resources in Karamay," *Ground Water* **38**(2), 126–129 (2016).
25. H. An, D. E. Green, and J. Johrendt, "Multi-objective optimization and sensitivity analysis of tube hydroforming," *Int. J. Adv. Manuf. Technol.* **50**, 67–84 (2010).

Guang Liu is a PhD candidate at the University of Chinese Academy of Sciences. His current research interests include space optical systems and thermal-structural-optical integrated analysis.

Liang Guo is a professor at the Changchun Institute of Optics, Fine Mechanics and Physics, Chinese Academy of Sciences. His research interests include heat and mass transfer, thermal-structural-optical integrated analysis, and precise thermal control technology.

Xintong Wang is a master candidate at the University of Chinese Academy of Sciences. Her current research interests include space optical systems and active optics.

Qingwen Wu is a professor at the Changchun Institute of Optics, Fine Mechanics and Physics, Chinese Academy of Sciences. His research interests include space optical remote sensing technology, thermal design and thermal control technology.